LETTERS
https://doi.org/10.1038/s41565-021-01062-4

nature nanotechnology

Industrial scale production of fibre batteries by a solution-extrusion method

Meng Liao[1,4], Chuang Wang[1,4], Yang Hong[1,4], Yanfeng Zhang[1], Xunliang Cheng[1], Hao Sun[1], Xinlin Huang[1], Lei Ye[1], Jingxia Wu[1], Xiang Shi[1], Xinyue Kang[1], Xufeng Zhou[1], Jiawei Wang[1], Pengzhou Li[1], Xuemei Sun[1], Peining Chen[1], Bingjie Wang[1] ✉, Yonggang Wang[2], Yongyao Xia[2], Yanhua Cheng[3] and Huisheng Peng[1] ✉

Fibre batteries are of significant interest because they can be woven into flexible textiles to form compact, wearable and light-weight power solutions[1,2]. However, current methods adapted from planar batteries through layer-by-layer coating processes can only make fibre batteries with low production rates, which fail to meet the requirements for real applications[2]. Here, we present a new and general solution-extrusion method that can produce continuous fibre batteries in a single step at industrial scale. Our three-channel industrial spinneret simultaneously extrudes and combines electrodes and electrolyte of fibre battery at high production rates. The laminar flow between functional components guarantees their seamless interfaces during extrusion. Our method yields 1,500 km of continuous fibre batteries for every spinneret unit, that is, more than three orders of magnitude longer fibres than previously reported[1,2]. Finally, we show a proof-of-principle for roughly 10 m^2 of woven textile for smart tent applications, with a battery with energy density of 550 mWh m^{-2}.

Reliance on mobile-operated systems in phones and electric vehicles has driven the demand for compact, light-weight and flexible power solutions, which are expected to replace current flat, rigid and bulky batteries[3–5]. Because fibres are so common in daily life (they are in the clothes we wear and carpets we walk on), incorporating energy-storage capabilities into a fibre that can then be woven into usable textiles is particularly attractive for wearable and mobile applications[6,7]. We envision a future where batteries can be worn like clothes and used to power a myriad of electronic devices.

Fibre batteries have been produced using methods adapted from planar batteries, where conductive and active materials and the electrolyte are coated layer-by-layer onto curved fibre substrates[8–13]. We further realized long fibre battery by revealing the relationship between battery performance and length[8]. However, the coating speeds on fibre substrates are typically low with production rates of <0.5 m min^{-1}. It is difficult to form thin and uniform active layers as required at much higher speeds at industry because this produces too many defects inside fibres, making them unsuitable for any meaningful applications[2].

Industrial production of chemical fibres from polymer melts or solutions are typically based on the use of technologies such as melt-drawing and solution-extruding methods, which may shed light on providing a solution to the above problem. Melt-drawing, which requires high temperatures to pull building materials at or above their softening temperatures, will decompose the active materials and volatize the electrolytes to cause compromised performance of the fibre battery. Solution extrusion is a potential alternative because the process conditions are mild and more suitable for mass production with high production rates. The problem with current solution-extrusion technology lies in that it generally produces single fibre components[14–17]. Using solution extrusion to produce a full fibre battery in a single step has not been achieved so far because accurately controlling the composition, microstructure and shape of the extruded fibre to obtain a seamless interface between the components for a battery is very challenging.

We present a new solution-extrusion method that can directly and continuously manufacture full fibre batteries in a single step at scale with high production rates over 250 m h^{-1}. We designed a single-unit industrial spinneret with three channels to extrude a three-component fibre battery consisting of parallel cathode and anode encapsulated by an electrolyte (Fig. 1a). The extruded fibre batteries are subsequently pulled, dried and collected on a winding spool ready for weaving into textiles (Fig. 1b–d). Because such a solution-extrusion regime does not require strict production conditions (for example, vacuum environment and high temperature), it is suitable for large-scale and high-rate production and can be used to make a variety of fibre batteries.

The process begins with the preparation of cathode, anode and gel electrolyte inks (see Supplementary Table 1 for details). To obtain inks with high apparent viscosities between 10^1 to 10^2 Pa s at a shear rate of 1 s^{-1}, we used high concentrations of solid materials (>300 mg ml^{-1}) to prepare the inks (Supplementary Fig. 1). Such a high apparent viscosity enhances spinnability and is conducive for continuous production of the fibre batteries[18]. Further, we prepared three inks with similar viscosities (Supplementary Fig. 2) to avoid their mixture during extrusion[19].

To make aqueous fibre lithium-ion batteries (FLIBs), we blended LA133 acrylonitrile binders with an aqueous dispersion of carbon nanotubes (CNTs) and obtained a slurry that formed the base component of the electrode ink with suitable viscosity for extrusion. Cathode inks were made by adding lithium manganese oxide to the slurry while anode inks were obtained by adding lithium titanate

---

[1]State Key Laboratory of Molecular Engineering of Polymers, Department of Macromolecular Science and Laboratory of Advanced Materials, Fudan University, Shanghai, China. [2]Department of Chemistry and Shanghai Key Laboratory of Molecular Catalysis and Innovative Materials, Institute of New Energy, iChEM (Collaborative Innovation Center of Chemistry for Energy Materials), Fudan University, Shanghai, China. [3]State Key Laboratory for Modification of Chemical Fibers and Polymer Materials, College of Materials Science and Engineering, Donghua University, Shanghai, China. [4]These authors contributed equally: Meng Liao, Chuang Wang, Yang Hong. ✉e-mail: wangbingjie@fudan.edu.cn; penghs@fudan.edu.cn

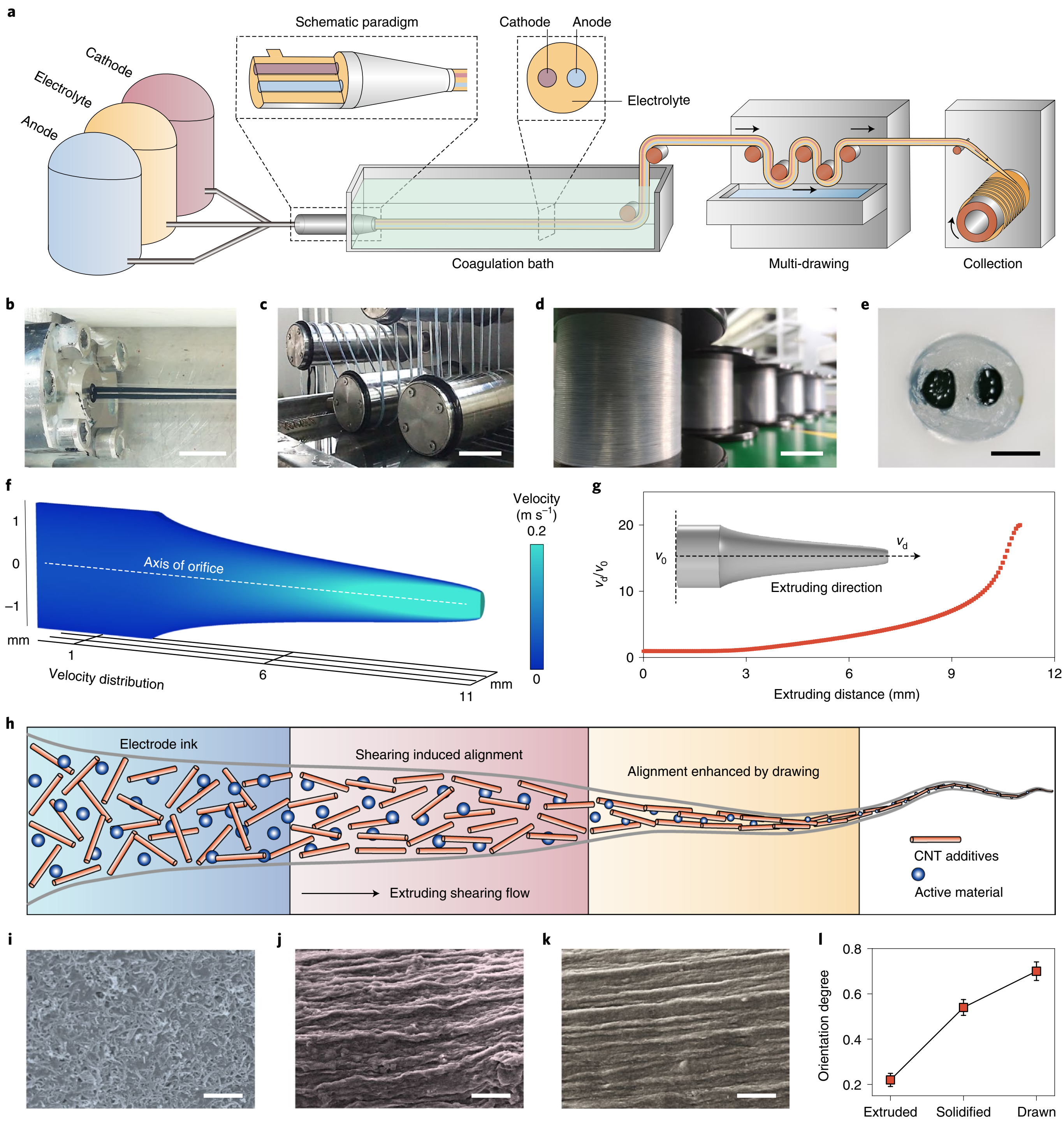

Fig. 1 | Extrusion process and structural characterization of fibre batteries. **a**, Schematic showing the setup for producing fibre batteries. Anode, cathode and electrolyte inks are simultaneously extruded from a tapered three-channel spinneret into a coagulation bath (containing 1.75 M NaOH and 2 M Li_2SO_4 solution), where the gel electrolyte coagulates around the anode and cathode fibres. Fibre batteries are subsequently washed, pulled, dried and collected on a winding spool at 2.5 m min^{-1}. **b**–**d**, Photographs of the fibre battery during extrusion (**b**), drawing (**c**) and collection (**d**). **e**, Cross-section photograph of a fibre battery shows both cathode and anode fibres (black) are uniformly spaced within the electrolyte (clear). **f**, Finite element simulation of a tapered channel for fibre electrode extrusion shows a much higher flow velocity distribution near the channel exit. **g**, Flow velocity is the highest at the channel exit. Extruding distance is the distance between the entrance and exit of the tapered channel. **h**, Schematic shows shear force during extrusion and drawing aligns one-dimensional nanomaterials such as CNTs in the inks. **i**–**k**, SEM images show random CNTs before extrusion (**i**) become more aligned after extrusion (**j**) and further drawing (**k**). **l**, Orientation degree of extruded, solidified and drawn fibre batteries. Raman analysis shows the orientation of CNTs in **i**–**k** increased from 0.2 to 0.7 on extrusion and drawing. Error bars represent the standard deviations of the results from five samples. Scale bars, 5 mm in **b**, 5 cm in **c** and **d**, 200 μm in **e**, 1 μm in **i**, 10 μm in **j** and **k**.

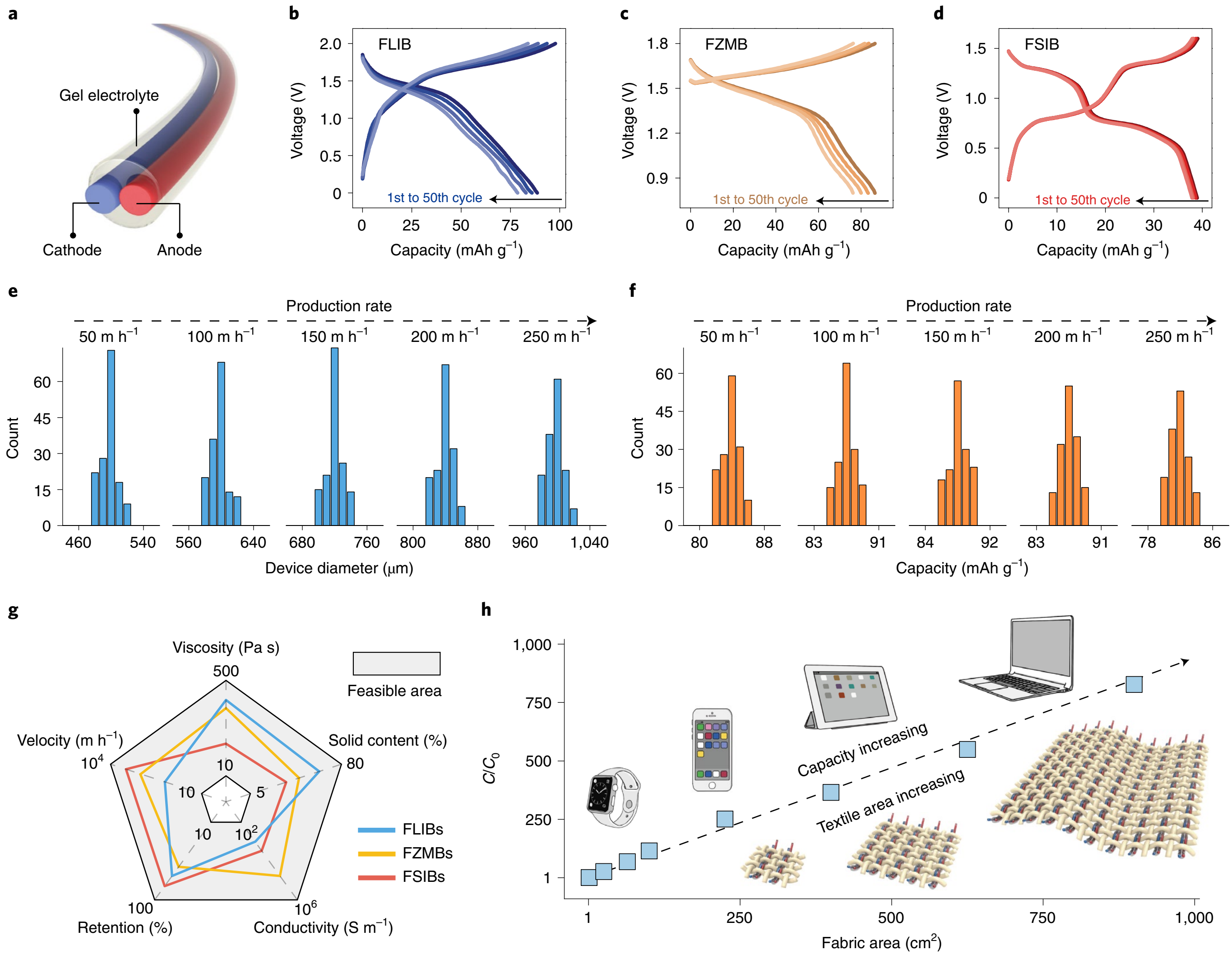

Fig. 2 | Continuous solution-extrusion method for producing aqueous Li-ion, Zn-Mn and Na-ion fibre batteries. a, Schematic of an extruded fibre battery. The three-component (cathode, anode and electrolyte) architecture is inherited from the spinneret structure. **b**–**d**, Typical charge and discharge profiles of aqueous FLIBs (**b**), aqueous fibre Zn-MnO$_2$ batteries (FZMBs) (**c**) and aqueous FSIBs (**d**) show the solution-extrusion method is general and effective. **e**,**f**, Both FLIB diameter (**e**) and specific capacity (**f**) showed <10% deviations at an increasing production rate from 50 to 250 m h^{-1}, indicating the solution-extrusion method is stable and compatible with high production rates. Measurements in **e** and **f** were made on 10-cm-long fibres obtained by cutting the extruded fibre batteries. Total of 150 samples were recorded at each production rate. **g**, Multi-angle comparison of production parameters for different types of extruded fibre battery provides the production criteria for extending the method to producing other types of fibre device. **h**, Experimental data showing discharge capacity of energy-storage textiles made from fibre batteries increased almost linearly with fabric area.

phosphate. A secondary binder (styrene butadiene rubber) was subsequently mixed into the respective electrode inks to enhance the flexibility of the extruded electrode fibres (Supplementary Fig. 3). Gel electrolyte inks were made by adding polyvinyl alcohol and lithium sulfate (Li$_2$SO$_4$) to chitosan in acetic acid. We used Li$_2$SO$_4$ as salt because it is compatible with a variety of active materials for batteries. Both the electrode and electrolyte inks obtained had a viscosity of roughly 20 Pa s (Supplementary Fig. 2c) and high laminar flow with a Reynolds number of <1 on extrusion (Supplementary Fig. 4).

To produce the fibre batteries, we first confirmed the electrochemical activities of our electrode and electrolyte inks by testing half cells and full cells using extruded fibre cathode, anode and electrolyte inks after encapsulation (Supplementary Fig. 5). The cells demonstrate similar behaviours to previously reported works[20–22], thus proving our inks remain fully functional on extrusion (Supplementary Fig. 6). Following that, the inks stored in three separate tanks were pumped through separate channels in the specially designed spinneret and simultaneously extruded into a coagulation bath containing lithium sulfate (Li$_2$SO$_4$) and sodium hydroxide (NaOH). The bath served to quickly solidify the gel electrolyte around the anode and cathode fibres through a deprotonation reaction, forming the full fibre battery architecture (Fig. 1a, see Supplementary Methods for details). Optical microscopy image of a 100-m long extruded fibre battery shows the cathode and anode fibres are uniformly spaced in both the transverse (Fig. 1e) and axial (Supplementary Fig. 7) directions. The spinneret structure could effectively combine electrodes and electrolyte in a single step to avoid the formation of non-uniform layers by a conventional coating method.

Besides ink composition, the key to continuous extrusion of fibres also lies in the design of the channels in the spinneret. Channels for the anode and cathode inks were designed to taper along the direction of extrusion (Supplementary Fig. 8a). As shown by finite element simulation, tapering concentrates the fluid flow of the electrode inks, rendering a 20-fold higher velocity (Fig. 1f,g) and a 30-fold enhanced shear force between the entrance and exit of the tapered channel (Supplementary Fig. 8b–d). This gradually increasing shear flow force along the extruding direction helps orient low-dimensional nanomaterials such as CNTs in the electrode inks (Fig. 1h)[23,24]. Both scanning electron microscopy (SEM) images (Fig. 1i–k) and further Raman analysis (Fig. 1l and Supplementary Fig. 9a) show initially random CNTs before extrusion gradually became more aligned after extrusion and further drawing. An increase in conductivity of the fibre electrode by roughly 20% further indicates alignment with a minimized device diameter (Supplementary Fig. 9b–d). Because charge transport in a fibre battery is along the axial direction, the highly aligned CNT network along the axial direction is expected to significantly reduce electrical resistance. Low electrical resistance for charge transport is key to fully using the energy-storage capabilities of the active materials in a battery[25,26].

Fibre batteries consisting of parallel cathode and anode fibres encapsulated by gel electrolytes are produced (Fig. 2a). Charge–discharge profiles of 10-cm-long extruded FLIBs demonstrate that these fibres are fully functional (Fig. 2b), displaying an average discharge potential plateau of 1.3 V, which is consistent with the corresponding cyclic voltammograms (Supplementary Fig. 6g). The full fibre battery delivered a specific capacity of 86 mAh g^{-1} at 50 mA g^{-1} and was stable over 50 cycles with a coulombic efficiency of 93.6%, outperforming some reported FLIBs (Supplementary Table 2 and Supplementary Fig. 10).

Our solution-extrusion method is general. Besides FLIBs, we produced aqueous fibre zinc-manganese dioxide batteries (FZMBs) using optimized cathode inks containing manganese oxide (MnO_2) and anode inks containing zinc (Zn) powder (Supplementary Fig. 10d–f). The charge–discharge profile of a 10-cm-long FZMB shows an initial capacity of roughly 88 mAh g^{-1} at 100 mA g^{-1} (Fig. 2c). In subsequent cycles, the capacity remained stable without any significant decay. The method can also produce aqueous fibre sodium-ion batteries (FSIBs). We used $Na_{0.44}MnO_2$ and $NaTi_2(PO_4)_3$ in the cathode and anode inks, respectively (Supplementary Fig. 10g–i). Because these fibres use Na^+-containing aqueous solutions, they are compatible with cell-culture medium and are particularly promising for powering implantable electronics[27,28]. Ten-centimetre-long FSIBs showed a capacity of roughly 38 mAh g^{-1} at 5 mA g^{-1} for over 50 cycles (Fig. 2d). Extruded aqueous fibre batteries also demonstrated capacity retention of >80% over 200 cycles (Supplementary Fig. 11). The bulk resistivity of the electrode fibres remained nearly unchanged for the long fibre battery (varied below 6%). This paves the way for solution extrusion to be a general strategy for large-scale production of fibre batteries.

The method has a high production rate for industrial setup, typically up to 250 m h^{-1} as the volumetric flux of the electrode inks and gel electrolyte is increased up to 42 ml min^{-1} (Supplementary Fig. 12a,b). The production rate can be amplified to industrial scale by increasing the number of extruding units in the spinneret (Supplementary Fig. 12c,d and Supplementary Video 1). Furthermore, the fibre batteries produced were highly reproducible. We cut the extruded fibres into 10-cm-long units and compared 150 units of fibre batteries at each production rate; both the diameter of the fibre (Fig. 2e) and specific capacity (Fig. 2f) showed narrow deviations <10% when the production rate increased from 50 to 250 m h^{-1}. The fibre batteries were highly flexible (Supplementary Fig. 13) and could withstand 10,000 cycles of bending with negligible mechanical and electrochemical decay (Supplementary Fig. 14a,b). The interfaces in extruded fibre batteries remained stable after bending, knotting and twisting (Supplementary Figs. 15 and 16). Moreover, the diameter of the extruded fibre batteries can be tweaked (from micrometres to millimetres) to suit the requirements of various applications (Supplementary Fig. 17). We further defined the fibre materials selection criteria and preparation parameters that are feasible for scalable production in Fig. 2g. The capacity of the extruded fibre batteries could potentially be further enhanced by synthesizing new active materials that are amenable to extrusion. Besides batteries, our extrusion method can also be used to rapidly produce at scale many other electronic devices such as supercapacitors, light-emitting devices and sensors.

The voltage or capacity of the battery packs made from our fibre batteries can be conveniently adjusted by arranging the connections of the fibres, opening the door for tuneable energy demands. For example, three 10-cm-long FLIBs connected in series could triple the output voltage to 6.0 V (Supplementary Fig. 14c) while in parallel, the capacity tripled to 0.7 mAh (Supplementary Fig. 14d). Further, the absolute discharge capacity of a battery textile composed of fibre batteries increased linearly to roughly 40 mAh as the textile area increased to roughly 1,000 cm^2 (Fig. 2h). This capacity can power for example, a commercial smart bracelet for >10 days.

We used a commercial braiding machine (Fig. 3a) to weave the continuous FLIBs into a textile battery with an area of roughly 10 m^2 (Fig. 3b and Supplementary Fig. 18a,b). Because of the use of the intrinsically safe aqueous gel electrolyte, the resulting textile battery is deemed safe for various wearable applications (Supplementary Fig. 18c and Supplementary Videos 2 and 3). The textile battery was extremely stable (Fig. 3c and Supplementary Fig. 19); it worked effectively even when heated up to roughly 300 °C over a flame (Supplementary Fig. 18d and Supplementary Video 4) and punctured with a blade (Supplementary Fig. 18e and Supplementary Video 5). Because the aqueous gel electrolyte used is non-flammable, no leakage or explosions were observed. Further, the capacity of the textile battery varied by less than 10% when immersed in water, pressed with a heavy object, washed with soap or repeatedly hammered (Supplementary Fig. 18f–i, Supplementary Fig. 20 and Supplementary Videos 6 and 7).

Because these fibre batteries are flexible, safe and durable, we envisioned using them to build an integrated textile that can harvest, store and discharge energy (Fig. 3d–f and Supplementary Fig. 21). As proof-of-concept, we fabricated a tent, where the outer layer was composed of textile solar cells and the inner layer was composed of textile batteries (Fig. 3f,g). The tent can harvest energy from the sun during the day to charge the textile batteries on the inside (Fig. 3g). We show the charged textile batteries effectively

Fig. 3 | Applications of textile battery made from FLIBs. a, Schematic (left) and photographs (right) of a commercial braiding machine used to weave textile battery from aqueous FLIBs. **b**, Photograph of a large area (>10-m long and 0.6-m wide) textile battery illustrates large-scale production is feasible. **c**, Output voltage of the FLIB-based textile battery is insensitive to squeezing, sunshine, rain, pressure, hammering and washing. **d**, Photographs of energy-harvesting (textile solar cells), energy-storage (textile batteries) and display textile modules for the all-textile integrated system. **e**, Circuit diagram for the integrated textile system in **d** and **f**. **f**, Operating mechanism (left) and schematic illustration (right) of an integrated textile system in the form of a tent consisting of textile solar cells on the outside and textile batteries and textile display modules on the inside. Electron flow (arrows) occurs through conducting wires that connect the different textile modules. **g**, Photo-charging (red line) by textile solar cells and discharging curves (blue line) of the textile batteries. Inset photos, textile solar cells on the outside of the tent harvest energy from the sun during the day and store the harvested energy in the FLIB textile on the inside of the tent. Charged textile batteries power electronic devices inside the tent at night. **h**, Photograph shows the textile display (left arrow) and smart sound box (right arrow) are powered by the charged textile batteries (2.1 m^2) inside the tent, demonstrating the practical use of an integrated textile system. Scale bars, 2 cm in **d** and **h**.

powered a textile display and a smart sound box inside the tent (Fig. 3h and Supplementary Video 8).

In conclusion, we report a generalizable and scalable solution-extrusion method for making full fibre batteries at high production rates. The method is straightforward, and the flexible textile battery obtained is stable, durable and safe. We anticipate that this method will promote large-scale production and practical applications of fibre batteries for the next-generation electronics.

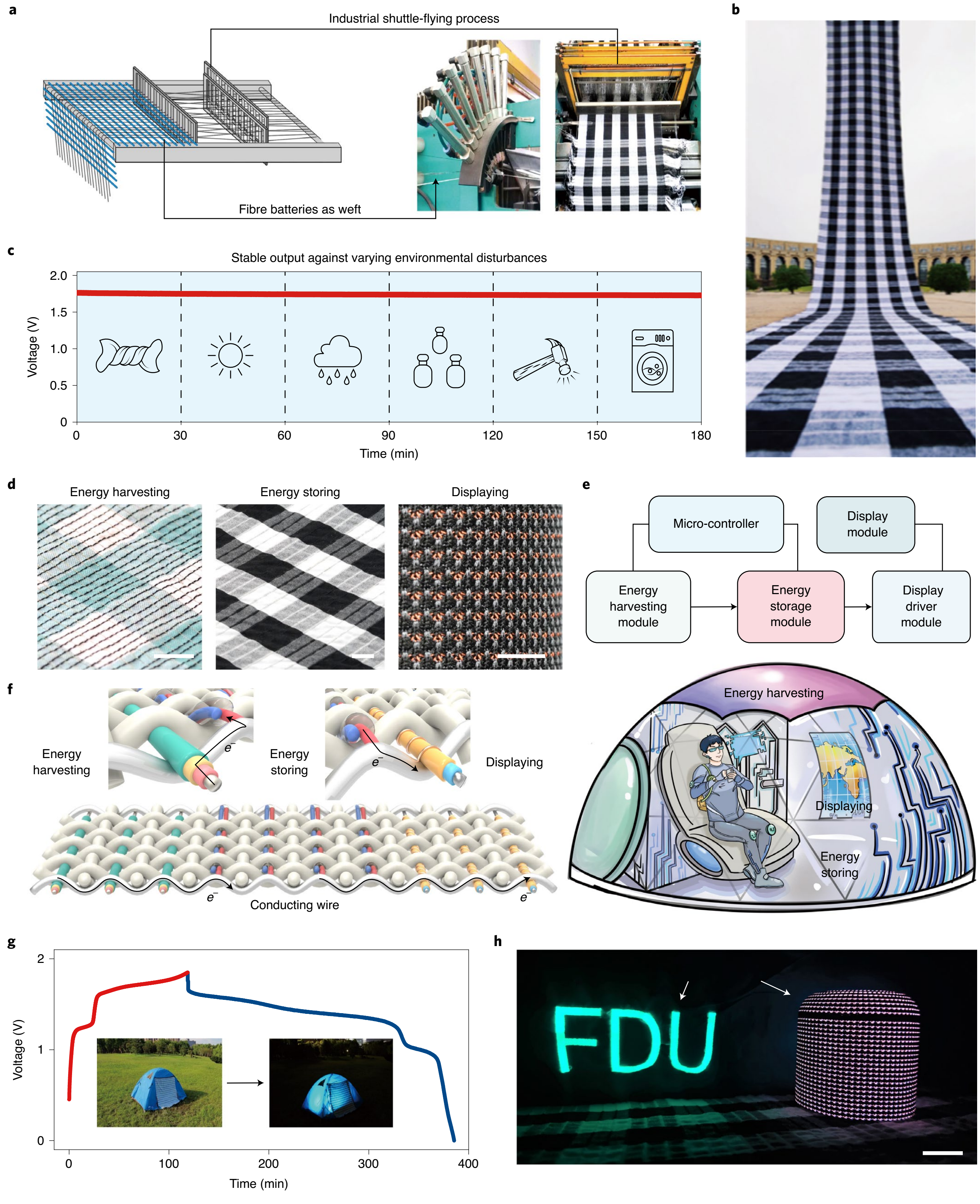

Online content

Any methods, additional references, Nature Research reporting summaries, source data, extended data, supplementary information, acknowledgements, peer review information; details of author contributions and competing interests; and statements of data and code availability are available at https://doi.org/10.1038/s41565-021-01062-4.

Received: 2 July 2021; Accepted: 25 November 2021;
Published online: 20 January 2022

References

1. Sun, H., Zhang, Y., Zhang, J., Sun, X. & Peng, H. Energy harvesting and storage in 1D devices. *Nat. Rev. Mater.* **2**, 17023 (2017).
2. Wang, L. et al. Application challenges in fiber and textile electronics. *Adv. Mater.* **32**, 1901971 (2020).
3. Park, S. et al. Self-powered ultra-flexible electronics via nano-grating-patterned organic photovoltaics. *Nature* **561**, 516–521 (2018).
4. Pomerantseva, E., Bonaccorso, F., Feng, X., Cui, Y. & Gogotsi, Y. Energy storage: the future enabled by nanomaterials. *Science* **366**, eaan8285 (2019).
5. Wang, S. et al. Skin electronics from scalable fabrication of an intrinsically stretchable transistor array. *Nature* **555**, 83–88 (2018).
6. Mo, F. et al. An overview of fiber-shaped batteries with a focus on multifunctionality, scalability, and technical difficulties. *Adv. Mater.* **32**, 1902151 (2020).
7. Chen, J. et al. Micro-cable structured textile for simultaneously harvesting solar and mechanical energy. *Nat. Energy* **1**, 16138 (2016).
8. He, J. et al. Scalable production of high-performing woven lithium-ion fibre batteries. *Nature* **597**, 57–63 (2021).
9. Zhu, Y. H., Yang, X. Y., Liu, T. & Zhang, X. B. Flexible 1D batteries: recent progress and prospects. *Adv. Mater.* **32**, 1901961 (2020).
10. Mackanic, D. G., Kao, M. & Bao, Z. Enabling deformable and stretchable batteries. *Adv. Energy Mater.* **10**, 2001424 (2020).
11. Kwon, Y. H. et al. Cable-type flexible lithium ion battery based on hollow multi-helix electrodes. *Adv. Mater.* **24**, 5192–5197 (2012).
12. Ren, J. et al. Twisting carbon nanotube fibers for both wire-shaped micro-supercapacitor and micro-battery. *Adv. Mater.* **25**, 1155–1159 (2013).
13. Guo, Z. et al. Multi-functional flexible aqueous sodium-ion batteries with high safety. *Chem* **3**, 348–362 (2017).
14. Yang, H. S. et al. Electrochemical wet-spinning process for fabricating strong PAN fibers via an in situ induced plasticizing effect. *Polymer* **202**, 122641 (2020).
15. Kinloch, I. A., Suhr, J., Lou, J., Young, R. J. & Ajayan, P. M. Composites with carbon nanotubes and graphene: an outlook. *Science* **362**, 547–553 (2018).
16. Li, P. et al. Highly crystalline graphene fibers with superior strength and conductivities by plasticization spinning. *Adv. Funct. Mater.* **30**, 2006584 (2020).
17. Wang, Y. et al. 3D-printed all-fiber Li-ion battery toward wearable energy storage. *Adv. Funct. Mater.* **27**, 1703140 (2017).
18. Rao, R. B., Krafcik, K. L., Morales, A. M. & Lewis, J. A. Microfabricated deposition nozzles for direct-write assembly of three-dimensional periodic structures. *Adv. Mater.* **17**, 289–293 (2005).
19. Kaufman, J. J. et al. Structured spheres generated by an in-fibre fluid instability. *Nature* **487**, 463–467 (2012).
20. Zhang, Y. et al. A fiber-shaped aqueous lithium ion battery with high power density. *J. Mater. Chem. A.* **4**, 9002–9008 (2016).
21. Chen, L. et al. Enabling safe aqueous lithium ion open batteries by suppressing oxygen reduction reaction. *Nat. Commun.* **11**, 2638 (2020).
22. Yang, C. et al. Aqueous Li-ion battery enabled by halogen conversion–intercalation chemistry in graphite. *Nature* **569**, 245–250 (2019).
23. Zhao, C. et al. Layered nanocomposites by shear-flow-induced alignment of nanosheets. *Nature* **580**, 210–215 (2020).
24. Liu, L. et al. Aligned, high-density semiconducting carbon nanotube arrays for high-performance electronics. *Science* **368**, 850–856 (2020).
25. Zhu, C., Usiskin, R. E., Yu, Y. & Maier, J. The nanoscale circuitry of battery electrodes. *Science* **358**, eaao2808 (2017).
26. Zhu, M. & Schmidt, O. G. Tiny robots and sensors need tiny batteries—here's how to do it. *Nature* **589**, 195–197 (2021).
27. Bin, D. et al. Progress in aqueous rechargeable sodium-ion batteries. Adv. Energy Mater. 8, 1703008 (2018).
28. Suo, L. et al. 'Water-in-salt' electrolyte makes aqueous sodium-ion battery safe, green, and long-lasting. *Adv. Energy Mater.* **7**, 1701189 (2017).

Methods

Methods and any associated references are available in the Supplementary Information.

Data availability

The data that support the findings of this study are available from the Supplementary Information or the corresponding authors on request. Source data are provided with this paper.

Acknowledgements

This work was supported by the Ministry of Science and Technology of the People's Republic of China (grant no. 2016YFA0203302 to H.P.), National Natural Science Foundation of China (grant nos. 21634003 to H.P., 22075050 to X. Sun, 21805044 to P.C.), Science and Technology Commission of Shanghai Municipality (grant nos. 20JC1414902 to H.P., 18QA1400700 to B.W., 19QA1400800 to P.C.) and Shanghai Municipal Education Commission (grant no. 2017-01-07-00-07-E00062 to H.P.). We thank A.-L. Chun of Science Storylab for critically reading and editing the manuscript and Y. Zhang for important suggestions.

Author contributions

H.P. and B.W. conceived and designed the research project. M.L., C.W. and Y.H. performed the experiments on solution-extruded fibre batteries, textile batteries and integration systems, and contributed equally to this work. Y.Z., X.C., H.S. and L.Y. performed electrochemical measurements of functional inks. X.H. performed the simulation. J. Wu, X. Shi and X.Z. performed experiments on the display textile. X.K. performed the experiments on the photovoltaic textile. J. Wang and P.L. analysed the data. X. Sun, P.C., Y.W., Y.X., Y.C. and all other authors discussed the data and wrote the paper.

Competing interests

The authors declare no competing interests.

Additional information

Supplementary information The online version contains supplementary material available at https://doi.org/10.1038/s41565-021-01062-4.

Correspondence and requests for materials should be addressed to Bingjie Wang or Huisheng Peng.

Peer review information *Nature Nanotechnology* thanks Sheng Yong, Xinbo Zhang and the other, anonymous, reviewer(s) for their contribution to the peer review of this work.

Reprints and permissions information is available at www.nature.com/reprints.